JGR Biogeosciences

Climate, Fuel, and Land Use Shaped the Spatial Pattern of Wildfire in California's Sierra Nevada

Bin Chen[1] , **Yufang Jin[1]** , **Erica Scaduto[1], Max A. Moritz[2], Michael L. Goulden[3], and James T. Randerson[3]**

[1]Department of Land, Air and Water Resources, University of California, Davis, CA, USA, [2]University of California Cooperative Extension Division of Agriculture and Natural Resources & Bren School of Environmental Science & Management, Santa Barbara, CA, USA, [3]Department of Earth System Science, University of California, Irvine, CA, USA

Abstract California's Sierra Nevada has experienced a large increase in wildfire activities over recent decades. This intensifying fire regime has coincided with a warming climate and increasing human activity, but the relative importance of the biophysical and anthropogenic drivers of wildfire remains unclear across this diverse landscape, especially at a finer spatial scale. We used multisource geospatial data sets of fire occurrence, and human, climatic, and biophysical variables to examine the spatial pattern and controls on Sierra Nevada wildfires averaged from 1984 to 2017. The maximum entropy model driven by both biophysical and anthropogenic variables predicted the spatial distribution of fire probability well, with an area under the curve (AUC) score of 0.81. Model diagnostics revealed that aspects of the climate, including vapor pressure deficit (VPD), temperature, and burning index (difficulty of control), dominated the spatial patterns of fire probability across the whole Sierra Nevada region. The VPD was the leading control, with a relative contribution of 32.1%. Population density and fuel amount were also significant drivers, each accounting for 15.8%–12.4% of relative contribution. VPD and burning index were the most important factors for fire probability in higher elevation forest, while population density was comparatively more important in the lower elevation forest regions of the Sierra Nevada. Our findings improved our understanding of the relative importance of various factors in shaping the spatial patterns of historical fire probability in the Sierra Nevada and across various subecoregions, providing insights for targeting spatially varying forest management strategies to limit potential future increases in wildfires.

1. Introduction

The increasing trend in western US wildfire extent and severity since the mid-1980s is threatening lives, properties, biodiversity, carbon sequestration, water and air quality, and other socioecological services (Moritz et al., 2014; Restaino & Peterson, 2013; Spracklen et al., 2007; Westerling, 2016; Westerling et al., 2006). California's Sierra Nevada ecoregion is a key source of water, electrical power, forest, and other natural resources to the state (Dettinger et al., 2018). The Sierra Nevada has experienced a series of catastrophic wildfire in recent decades (Miller & Safford, 2012; Peterson et al., 2015), coincident with spring and summer warming due to climate change (Westerling et al. 2003, 2006), increasingly extreme fire weather (Keyser & Westerling, 2019; Stephens et al., 2018), forest densification due to fire suppression (Collins & Stephens, 2007), increasing population (Balch et al., 2017), and expanding human development (Syphard et al. 2007, 2019).

The Sierra Nevada ecoregion is characterized by a wide elevation range, complex topography, spatially variable climate, and diverse vegetation. Fire regimes and their environmental controls vary with elevation (Caprio & Swetnam, 1995; Schwartz et al., 2015), and are closely tied to vegetation types regulated by climate (Miller et al. 2009, 2012). The historic fire frequency from 1700 to 1900 was inversely related to elevation (Swetnam et al., 1998), with low severity but frequent fires in lower elevation foothill ecosystems, and high intensity but infrequent fires at higher elevations. This heterogeneous distribution of fire risk underscores the importance of better understanding the spatial pattern and drivers of wildfire occurrence.

Wildfire occurrence is regulated by interactions between ignition and climate, weather, fuel structure and composition, and topography (Mansuy et al., 2019; Parisien & Moritz, 2009). Areas with favorable meteorological and vegetation conditions may not necessarily experience frequent fires if ignitions are infrequent. Wildfires occur and expand under suitable environmental conditions, including the co-occurrence

of adequate fuel loads, and dry, warm or windy weather conducive to combustion and spread (Parisien & Moritz, 2009). These conditions vary in space and time in the Sierran landscape, resulting in heterogeneous patterns of wildfire occurrence and severity.

Human activities also play a central role in wildfire occurrence (Butsic et al., 2015; Mann et al., 2016; Syphard et al. 2007, 2019). Human activities and land use alter the wildfire regime through deliberate or accidental ignitions, suppression, fuel alteration including vegetation treatments, prescribed fire, forest clearing, and cultivation, as well as fuel continuity and landscape fragmentation (Balch et al., 2017; Radeloff et al., 2005; Syphard et al., 2019). The population living in or near areas of natural vegetation continues to increase, creating areas known as the wildland-urban interface (WUI; Radeloff et al., 2005). The expanding WUI leads to increasing road and trail density and traffic (Radeloff et al., 2018). Syphard et al. (2007) found a highly significant relationship between fire frequency and indices of human settlement such as population density and distance to WUI at the county level in California. The structure of human development in the WUI and the interaction with vegetation are important risk factors for fire. Areas of interface WUI, where development is adjacent to wildland vegetation, have a lower fire probability than areas of intermix WUI, where development is intermingled with wildland vegetation (Haight et al., 2004; Syphard et al., 2007). Increases in electrical infrastructure and transmission lines with WUI expansion create further ignition risk, especially under extreme weather conditions (Calkin et al., 2014; San-Miguel-Ayanz et al., 2013). For example, California's 2018 Camp fire was caused by arcing transmission lines owned by Pacific Gas & Electric (PG&E; Sullivan et al., 2019); the co-occurrence of strong wind, low humidity, and warm temperatures contributed to both the fire's ignition and extreme rate of spread (Brewer & Clements, 2020).

Both climate and human activities are expected to continue changing in the coming decades (Miller et al., 2012; Pechony & Shindell, 2010; Parisien et al., 2016; Syphard et al., 2019). An improved understanding of their effects on the spatial pattern of wildfire is critical for identifying the most vulnerable areas and predicting how the patterns of fire may evolve. Despite recent advancement in this field, several important challenges remain. Previous studies have mostly focused on very coarse spatial scales, at either state or continental levels (Mansuy et al., 2019; Parisien & Moritz, 2009; Parisien et al., 2016). Parisien and Moritz (2009) examined environmental controls on the distribution of wildfire using climate, vegetation type and topographic predictors. Parisien et al. (2016) extended this analysis, and found that variables that describe human activities are also important for predicting fire. Mansuy et al. (2019) used burned areas from 1984 to 2014 and 11 anthropogenic, climatic, and physical predictors to model fire likelihood inside and outside of protected areas in North America. They found that climate variables are especially important for explaining the spatial pattern of fire activity, while anthropogenic variables are of secondary importance. The influences of biophysical and anthropogenic variables on wildfire activities at finer spatial scales, however, is critically important for developing strategies and actions for effective fire management, but has not been fully addressed. The findings from the whole Sierra Nevada region (e.g., Parisien & Moritz, 2009) may not be applicable locally, because the localized wildfire controls may vary across subecoregions. Moreover, a comprehensive list of possible biophysical and anthropogenic predictors for the spatial variability in fire probability have not been fully explored in a systematic way. For example, metrics of human activities have largely been limited to population-related variables, although recently a few studies have incorporated some aspects of transportation, electrical infrastructure, and human footprints (Fusco, 2016; Pairisen et al., 2012; Whitman et al., 2015). The relative importance of biophysical and anthropogenic influences and how they vary across subecoregions remain less clear.

We explored the drivers shaping contemporary wildfire occurrence in the Sierra Nevada at a 4-km gridded scale, using a comprehensive set of multisource geospatial data layers, including explicit information on climate, fuel, human settlement, transportation, and electrical infrastructure. An improved understanding of this issue is needed to guide the spatially varying management of fire-dependent ecosystems in the face of ongoing and future climate change. Our analysis used the maximum entropy statistical approach, to address the following questions: (1) How do biophysical and anthropogenic controls contribute to the finer-scale spatial patterns of wildfire probability in the Sierra Nevada? (2) What is the relative importance of fuels, weather, topography and humans? (3) Do human-climate-vegetation-wildfire relationships vary across different subecoregions?
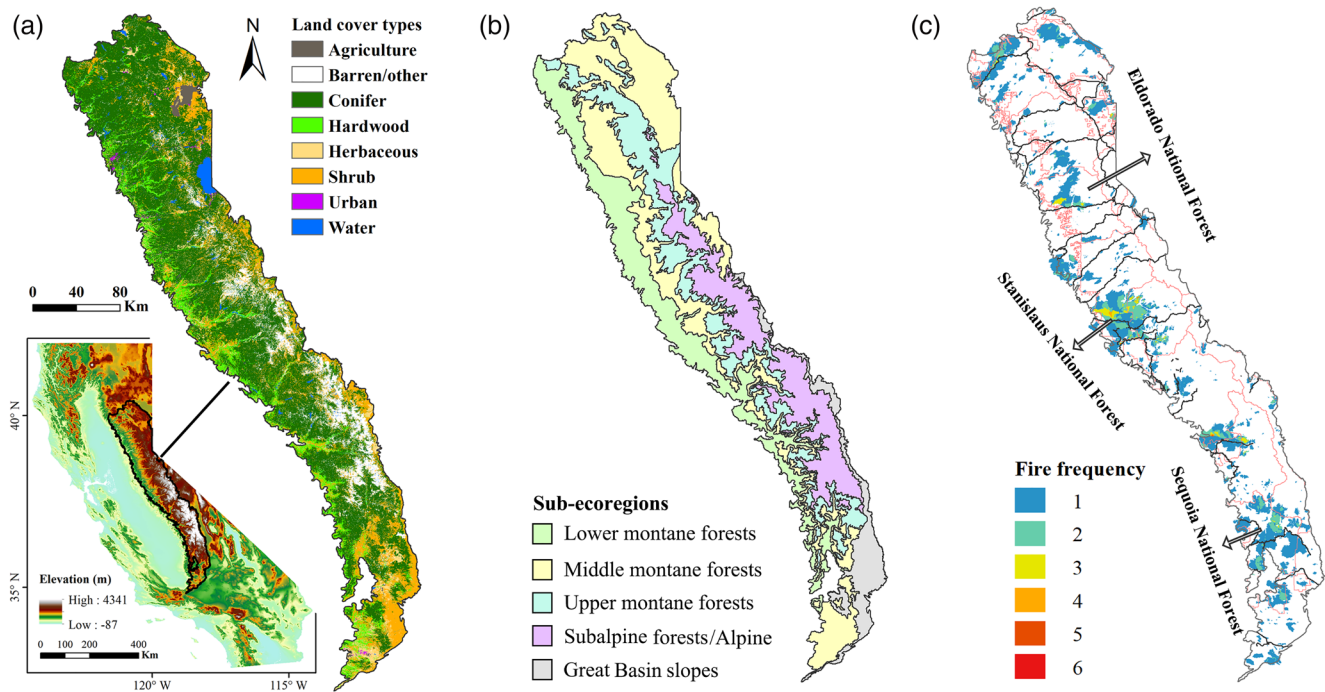
Figure 1. The Sierra Nevada study area: (a) vegetation type from FRAP's 2015 land cover map, (b) subecoregion divisions based on California's Level III ecoregions and vegetation classification zones (US Forest Service, 2009), and (c) fire frequency from 1984 to 2017 overlaid with major roads (black lines) and national forest boundaries (pink lines). FRAP, Fire and Resource Assessment Program.

2. Data and Methods

2.1. Study Area

We focus on the entire Sierra Nevada, a mountain range in eastern California that runs 640 km north-to-south and 110 km east-to-west (Figure 1a). Our study boundary was based on California's Level III ecoregions and vegetation classification zones (US Forest Service, 2009), encompassing 51,035 km^2 and including five subecoregions: lower montane forests, middle montane forests, upper montane forests, subalpine forests and alpine, and Great Basin slopes (Figure 1b). The region has a Mediterranean climate, with cool, moist winters and warm, dry summers (Goulden et al., 2012). The vegetation varies with altitude, from shrubs and herbs at lower elevations, to conifer woodlands and forests at middle and higher elevations (Figure 1a).

2.2. Fire History Data

We used the statewide GIS layer of fire perimeters from the California Fire and Resource Assessment Program (FRAP; version 17_1; California Department of Forestry and Fire Protection, 2017) for burned area history. Fires greater than 10 acres (~4 hectares) have been compiled by the California Department of Forestry and Fire Protection, USDA Forest Service Region 5, National Park Service, and other agencies since 1950. This data set represents the most complete digital record of fire history in California and has been updated annually. Each entry includes the final fire perimeter, dates of discovery and control, and cause. We focused on all nonprescribed and nonfirefighter training fires that occurred within the full Sierra Nevada from 1984 to 2017, when the availability of Landsat observations improved the fire-perimeter quality and also enabled vegetation characterization. Our data set included 1,466 fires with a total burned area of 1.09 million hectares (i.e., 18.4% of the area) during the period (Figure 1c).

We generated a gridded burn probability map during 1984–2017 at a 4-km spatial resolution, which served as a baseline for selecting fire-presence points. We first rasterized the fire perimeter from the FRAP fire history to 30-m resolution to preserve spatial details from the original data set. For each 30-m by 30-m pixel, we

Table 1
List of Variables and Data Sets Used to Quantify Biophysical Controls in This Study

Type	Indicator (unit at 4-km)	Time period	Spatial resolution	Data source
Climate (long term annual mean)	Precipitation (mm/month)	1984–2017 (monthly)	4-km	PRISM (Daly et al., 2008)
	Temperature (°C)			
	Vapor pressure deficit (VPD) (hPa)			
	Dew point temperature (°C)			
	Palmer drought stress index (PDSI)	1984–2017	4-km	University of Idaho Palmer Drought Severity Index (Abatzoglou et al., 2014)
	Wind direction (degree clockwise from north)	1984–2017 (aggregated from daily to monthly mean)	4-km	GRIDMET (Abatzoglou, 2013)
	Wind velocity (m/s)			
	Relative humidity (%)			
	Specific humidity (Kg/Kg)			
	Surface downward shortwave radiation (W/m^2)			
	100 h/1000 h dead fuel moisture (%)			
	Fire danger index: burning index and energy release component			
	Lightning-strike density (number of strikes/16 km^2)	1988–2012	4-km	NOAA Vaisala National Lightning Detection Network (https://www.ncdc.noaa.gov)
Vegetation (long term annual mean)	Tree cover percentage (%)	2000–2015 (annual)	250-m	MODIS-MOD44B (DiMiceli et al., 2017)
	Net primary production (NPP) (kgC/m^2/year)		250-m	MODIS-MOD17A3 (Heinsch et al., 2003)
	Normalized difference vegetation index (NDVI)	1984–2017 (annual max)	30-m	Landsat-5/7/8
Topography	Elevation (m)	2010	250-m	Global multiresolution terrain elevation data (GMTED; Danielson and Gesch, 2011)
	Slope (degree)		250-m	

calculated how many times it got burned, that is, fire frequency, during 1984–2017. A total of 2.2 million pixels, 3.89% of the study area, experienced repeated burning. We therefore further averaged the fire frequency over all 30-m pixels within each 4-km grid, as a measure of burn probability, that is, fire-affected fraction of each 4-km grid cell, taking repeated burning into account, during the study period. This fire probability map represented the fire history at 4-km resolution. A total of 1,475 fire-affected grids, that is, fire probability >0, was found within the region's 3,310 grids, considering both annual burned area and fire frequency.

2.3. Meteorological Records

We used two data sets for meteorological variables during 1984–2017 (Table 1). We downloaded the Parameter-Elevation Regressions on Independent Slope Model (PRISM) meteorological data at 4-km resolution, which included monthly precipitation, temperature (max/min/mean), vapor pressure deficit (VPD) (max/min/mean), and dew point temperature (mean) (http://www.prism.oregonstate.edu/). PRISM extrapolates weather station observations using a digital elevation model (DEM) and other spatial data sets to create gridded estimates of weather and climate (Daly et al., 2008). We also used 4-km Palmer Drought Severity Index (PDSI), calculated over a 10-day period and then averaged from 1984 to 2017 (Figure S1), as a measure of historical meteorological drought events (Abatzoglou et al., 2014; Dai et al., 2004).

To quantify wind and other fire weather related characteristics, we used the Gridded Surface Meteorological data set (GRIDMET) at 4-km resolution (Abatzoglou, 2013). This data set blends the high resolution spatial

data from PRISM with the high temporal resolution data from the National Land Data Assimilation System (NLDAS) to produce spatially and temporally continuous fields of meteorological variables across the contiguous United States (Abatzoglou, 2013). For a more comprehensive investigation of climatic controls on wildfire probability, we used daily estimates of 10 m wind velocity and direction, affecting rate and direction of spread; relative and specific humidity, 100-h/1000-h dead fuel moisture, and surface downward short-wave radiation, which regulate fuel flammability and drying rate; and two composite fire danger indices, that is, energy release component (a composite fuel moisture index that reflects the contribution of all live and dead fuels to potential fire intensity) and burning index (a number describes the potential amount of effort needed to contain a single fire in a particular fuel type within a rating area to represent the difficulty of fire control).

To quantify the natural ignition pressure (e.g., lightning-strike density) on wildfire occurrence, we obtained 4-km gridded monthly lightning-strike data from the National Oceanic and Atmospheric Administration (NOAA) Vaisala National Lightning Detection Network (https://www.ncdc.noaa.gov/data-access/severe-weather/lightning-products-and-services) from 1988 to 2012. The majority of lightning strikes is clustered in summer, but there are still certain percentages of lightning in spring and fall (Figure S2). We here chose to include all lightning strikes over the whole year to represent the lightning stress.

All the short-term meteorological records were subsequently averaged to derive long-term annual means over the study period.

2.4. Vegetation and Topography

We derived annual maximum normalized difference vegetation index (NDVI) at 30 m from Landsat to quantify spatial differences in leaf area. The Landsat surface reflectance images were filtered using the cloud mask and quality assessment (QA) information in the Landsat metadata (Chen et al., 2019). NDVI values were then calculated from the retained reflectance in the red and near infrared (NIR) bands, and annual maximum NDVI was determined for each year. All of the satellite-based vegetation variables were aggregated to long-term annual means at 4-km to match the meteorological records.

We also used spatially explicit vegetation information derived from the Moderate Resolution Imaging Spectroradiometer (MODIS) during 2000–2015 and Landsat-5/7/8 during 1984–2017 (Table 1). The MODIS annual vegetation continuous fields (VCF) product (MOD44B) at 250 m was used to quantify percent tree cover (DiMiceli et al., 2017). The MODIS net primary production (NPP) product (MOD17A3) at 1 km was used as a proxy of carbon flow into fuels (Heinsch et al., 2003).

We used the global multiresolution terrain elevation data in 2010 (250-m GMTED2010) to extract elevation and calculate topographic slope gradients across the full Sierra Nevada (Danielson & Gesch, 2011). The biophysical variables used in this study are summarized in Table 1.

2.5. Anthropogenic Variables

We compiled a set of human predictors, including population density, human settlement, transportation, mining production, and electrical infrastructure from various sources (Table 2). These variables were aggregated to a spatial resolution of 4 km for a baseline year or for long-term annual means. The percentage of developed area within each 4-km grid was calculated based on the presence of built-up areas in the different epochs, that is, 1990, 2000, 2015, at the spatial resolution of 250 m from the global human settlement layer (GHSL); it was generated by combining fine-scale satellite imagery, census data, and volunteered geographic information (Pesaresi et al., 2016). Estimates of mean population density (people per square kilometer) came from the gridded population of the world (GPWv4) product at 1-km spatial resolution, available for 2000, 2005, 2010, and 2015. The mean values over the available epochs were calculated and aggregated to the same 4 km grids.

The road density (major, minor, trail, and rail roads) within each 4-km cell was calculated from the Open Street Map (OSM). Initiated in 2004 as a volunteer effort, OSM is now a substantial global spatial database that maps point, line, and polygon features (OpenStreetMap, 2017). The positional accuracy of OSM features (±20 m) was found to be higher than those from other publicly available global data sets such as

Table 2
List of Anthropogenic Variables and Data Sets Used in This Study to Quantify Human Controls

Stressor	Indicator	Unit at 4-km	Year	Resolution	Data source
Human settlement	Built-up areas	Percentage	1990,2000,2015	250-m	Global human settlement layer (GHSL)
	Population	Density	2000, 2005, 2010, 2015	1-km	Gridded population of the world version 4 (GPWv4)-population density
Transportation	Major roads	Density	2016	30–500 m	Open Street Map
	Minor roads				
	Two-track trails				
	Railroads				
Mining production	Mining	Density	2016	100 m	Open Street Map
Electrical infrastructure	Powerlines	Density	2016	30-m	Open Street Map
	Nighttime lights	Mean value	1992–2013	1-km	DMSP/OLS v4 stable light
Combination	Human modification	Percentage	2016	1-km	Global human modification data set (gHM)
	Travel time	Minute	2015	1-km	Travel time to nearest densely populated area product

Global Roads Open Access Data Set (±500 m; Haklay, 2010). We used the linear features of the OSM powerline layers, mostly overhead electrical transmission lines, and DMSP/OLS nighttime light images, separately, to quantify the density of electrical infrastructure. The OSM mining points were used to represent the influence of mining production. The travel time to nearest densely populated area was used as another measure of human accessibility (Weiss et al., 2018).

We used a composite human modification indicator from the Global Human Modification data set, which was based on modeling the physical extents of 13 anthropogenic stressors and their estimated impacts using spatially explicit global data sets for 2016 (Kennedy et al., 2019).

2.6. Statistical Modeling

We explored the spatial pattern of fire occurrence and predictors using the maximum entropy statistical method (MaxEnt v3.3.3k; Phillips et al., 2004, 2006), which has been widely used to model and predict wildfire probability (Moritz et al., 2012; Parisien & Moritz, 2009; Parisien et al. 2012, 2016).

MaxEnt is a machine-learning technique originally designed to model species distribution from presence-only data based on multidimensional environmental inputs (Phillips et al., 2004, 2006). It estimates a target probability distribution by iteratively searching for the probability distribution with maximum entropy (i.e., the one that is most uniform), subject to the environmental variables at each observation (i.e., presence-only point). It is suitable for fire occurrence data in this study, where "true absence" of fires is not known with high confidence. MaxEnt allows us to model highly complex relationships while avoiding overfitting by using l_1-regularization (Phillips et al., 2006). We included all explanatory variables without differentiating direct and indirect causes for building MaxEnt models.

The presence-only framework was used here to model fire probability by coupling a large suite of biophysical and anthropogenic variables in this study, based on the following two considerations: (i) a lack of fire occurrence over the period 1984–2017 might not be interpreted as a true absence in the past (i.e., before 1984); and (ii) presence-only and presence-absence frameworks have been shown to provide similar model accuracies of fire probability (Parisien & Moritz, 2009; Parisien et al., 2016). MaxEnt therefore evaluates the environmental space of the fire presence (i.e., 1) in contrast to that of the environmental background of the entire study area.

We drew fire presence samples from the 4 km fire probability map as described in Section 2.1. We chose 0.6 as the cut-off threshold to select fire-presence samples, to balance the confidence-level of the samples and the resulting total number of samples for modeling. This resulted in a total of 469 high-confidence

fire-presence samples, where more than 60% of 4-km grid areas were burned during 1984–2017. Sensitivity analysis of model performance to the cut-off thresholds was conducted as well (Table S1), for example, the thresholds of 0.06, 0.3, 0.6, 0.9, and 1 resulted in the presence samples ranging from 1,050, 685, 469, 307, and 130, respectively. Previous fire studies have typically selected fire-presence samples from the annual burned area using random sampling (Krawchuk & Moritz, 2014; Mansuy et al., 2019; Parisien & Moritz, 2009; Parisien et al., 2016). However, due to the large difference in spatial resolution between explanatory variables and fire-presence data, this sampling strategy may lead to redundancy from repeated sampling for large fires, and uncertainty for small fires (Supplementary materials; Figure S3).

The MaxEnt model was trained using a random subset of 75% of fire-presence samples, with the remaining 25% retained for independent out-of-sample testing. We initially created the model using the complete set of variables described above; we refer to this run as the "full" model. The variable importance was then quantified based on the increase in regularized gain of model performance associated with the addition of each variable (Phillips et al., 2006). Given that some of the important variables may be highly correlated, we also calculated the covariance among predictors. Instead of feeding all variables into MaxEnt models, we selected a subset of features or important variables for the subsequent modeling and analysis; we refer to this as the "selected" model. We chose only one representative variable from the same subgroup, for example, for temperature, one variable from max/min/mean temperature, based on variable importance. Hence, variables from different subgroups should be less-correlated with other variables among different subgroups (i.e., $r < 0.9$ for different classes of biophysical variables, and $r < 0.7$ for different classes of anthropogenic variables). We also compared the model performance after excluding highly correlated variables (i.e., selected model) with that derived using the full model.

We built three sets of MaxEnt models to examine the impacts of biophysical and anthropogenic variables on fire probability. The first set used only long term mean climate, vegetation, and topographical variables (hereafter "natural model"); the second set used only anthropogenic variables (hereafter "human model"), and the third one combined biophysical and anthropogenic variables as input (hereafter "integrated model"). We applied a similar procedure to each individual subecoregion to further explore the spatial variation in the controls on fire.

2.7. Model Performance and Analysis of Variable Contribution

The MaxEnt model run was repeated 100 times, that is, training the MaxEnt with randomly selected 75% of the presence-only samples and predicting burn probability for the corresponding 25% data (out-of-samples) each time. The mean statistics on the 25% testing data from each of the 100 ensembles were used as quantitative measures of model performance. We used the receiver operating characteristic (ROC) curve, which was created by plotting sensitivity (i.e., the proportion of observed presences correctly predicted) on the y-axis against "1-specificity" (i.e., the fractional predicted area) on the x-axis for all possible thresholds, to quantify the model performance.

Based on the ROC curves, we measured the area under the curve (AUC) value, expressed as proportion of the total area of the square defined by the axis. The AUC can be viewed as the probability that a random presence sample is correctly predicted by the model (Phillips et al., 2006). For example, an AUC value of 0.5 indicates where prediction accuracy is no better than if samples were randomly selected, while a value of 1 indicating where prediction is ideal. Models with AUC values above 0.75 are typically considered useful (Elith, 2000). It should be noted that since we only have presence data, no real absence data, we calculated AUC by distinguishing presence from random phenomenon, rather than presence from absence. The quantity "1-specificity," that is, the fraction of the total study area predicted as present, is used rather than the more standard commission rate (i.e., the fraction of absences predicted present).

We evaluated the variable importance in controlling the spatial pattern of wildfire probability during the MaxEnt training process. The relative contribution was quantified by the increase in regularized gain of including the corresponding variable while keeping all other explanatory variables at their average sample value (Phillips et al., 2006). When there are highly correlated variables used in the MaxEnt models, the contributions from each variable should be interpreted with caution. Therefore, we conducted a preselection of important variables to exclude highly correlated predictors as mentioned in Section 2.5. We further

examined how each variable affected burn probability using partial dependence plots, that is, the marginal response of fire occurrence probability to each variable, when all other explanatory variables are kept constant at their mean values (Phillips et al., 2004, 2006; Elith et al., 2011).

3. Results

3.1. Variable/Feature Selection

The full MaxEnt model with the complete set of predictors showed that biophysical variables predominantly control the spatial patterns of fire probability in the Sierra Nevada (Figure 2a). Except for population density, all other most important variables were related to climate, fuels, and topography. However, most of these biophysical variables were highly correlated (Figure 2b). For example, tree cover, NPP, and NDVI were highly correlated (i.e., $r > 0.9$). Based on the selection rules defined in Section 2.5, we chose a total of 10 representative biophysical variables. These variables included NPP, which we interpret as a proxy for fuels. The collinearities among anthropogenic variables were lower (Figure 2b), and we selected the top eight variables except for the human modification variable, which was correlated with nighttime light and minor roads. The 18 selected biophysical and anthropogenic variables are summarized in Table S2.

3.2. Model Performance for Predicting Fire Probability

The full model and integrated model, with both biophysical and anthropogenic predictors, performed well in capturing the spatial distribution of fire probability (Figures 3a–3c). Higher fire probability was mostly distributed in lower and middle montane forests. Higher elevation slopes such as those dominated by subalpine forests had much lower fire probability. Fire probability on the eastern, Great Basin slope of the ecoregion was also low. Compared with the full model using the complete set of explanatory variables (Figure 3b), the reduced model (integrated model) driven by the refined subset of biophysical and anthropogenic variables achieved comparable prediction performance (Figure 3c). When driven only by biophysical variables, the predicted fire probability had a similar spatial pattern (Figure 3d). In contrast, the model with anthropogenic variables only (Figure 3e) resulted in a more uniform prediction of fire probability. Large discrepancies in the distribution of fire probability were observed, especially at higher elevations. This is because fire-presence samples used in this study are integrated with both human- and lightning-caused ignitions. However, the majority of wildfires at high elevation are caused by lightning. The fire probability prediction driven by anthropogenic predictors alone was unrealistically uniform, thus leading to a large overestimation of Sierra-wide fire probability. Similarly, the individual subecoregion predictions driven by anthropogenic variables alone overestimated the large-scale fire probability (Figure S4).

The ROC curves showed an average AUC of 0.79 over the 100-replicate runs for the integrated model of fire probability as a function of both biophysical and anthropogenic variables (Figure 4b), which was slightly lower than that of the model using the complete set of explanatory variables (Figure 4a). In contrast, the model with only biophysical drivers (Figure 4c) achieved an AUC of 0.76. The anthropogenic model only achieved an AUC of 0.62 (Figure 4d) due to the large overestimation of fire probability in higher elevation slopes (Figure 3e).

### 3.3. Importance of Biophysical Variables

The long-term mean VPD was the most influential predictor of the spatial pattern of fire probability, with a relative contribution of 32.1% to the integrated model (Figure 5). The response of fire probability to VPD followed a "bell" curve, increasing rapidly at low VPD (especially between 4 and 8 hPa), and then decreasing at high VPD, as shown by the partial dependence plots (Figure 6a).

Net primary productivity (NPP), which is a proxy for fuel availability, was the second most important biophysical variables, with a relative contribution of 12.4% (Figure 5). Higher NPP typically led to higher fire probability (Figure 6c). The long-term mean maximum temperature was the third important biophysical

Figure 2. Variable importance and collinearities of explanatory variables. The relative contribution of variables to fire probability (a) was based on the out-of-sample predictions from the full MaxEnt model using the complete set of variables. The matrix of correlation coefficients among paired anthropogenic and biophysical variables is show in (b). All 18 selected variables were marked with *.
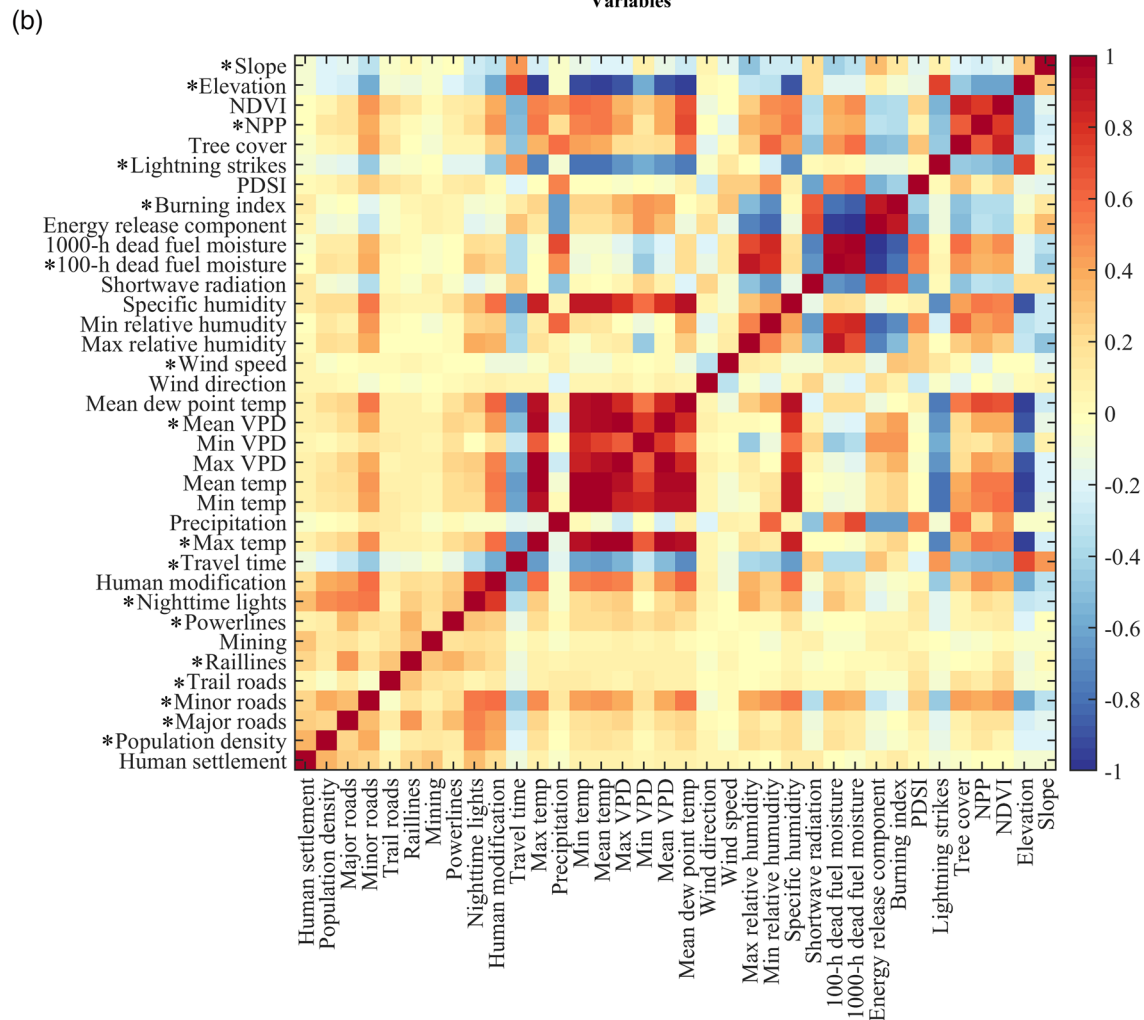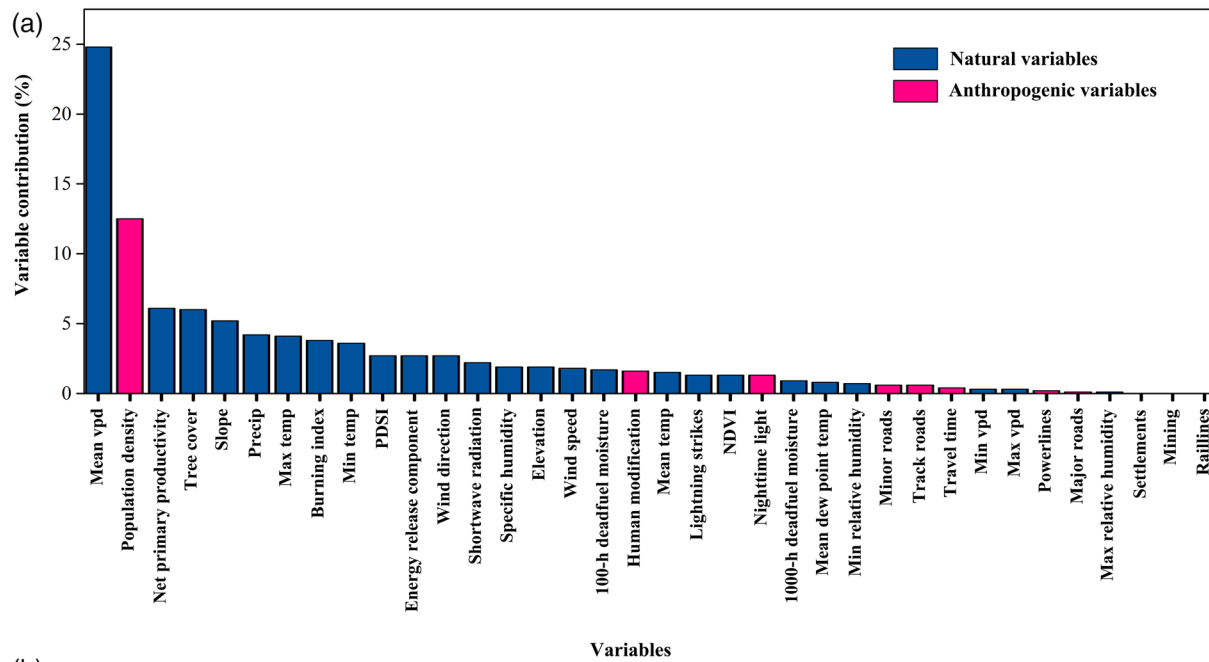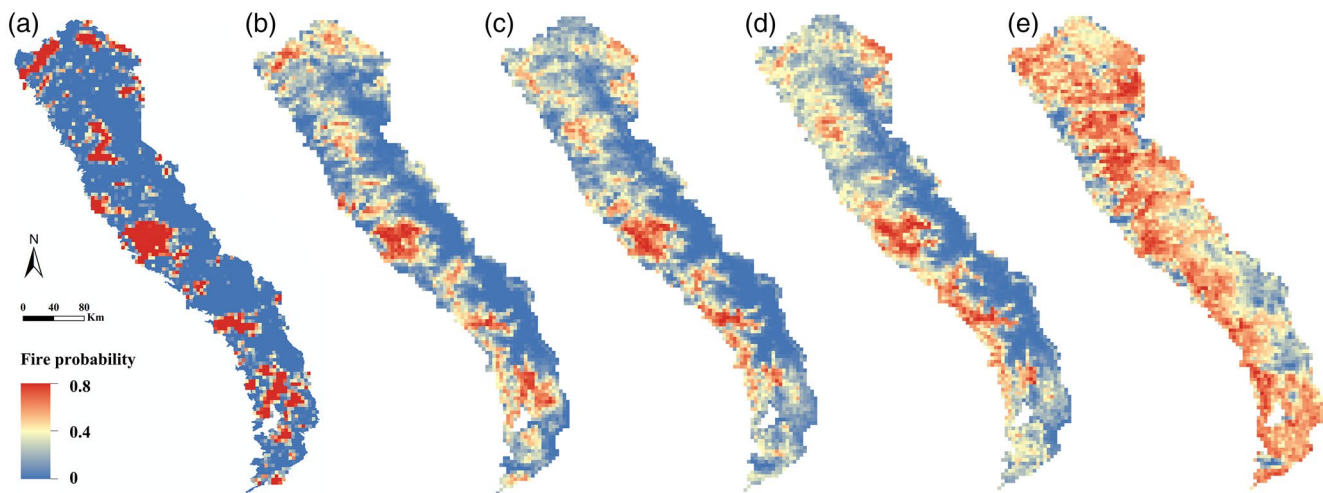
Figure 3. Fire probability in Sierra Nevada as derived from (a) FRAP (1984–2017) and predicted by MaxEnt models driven by (b) the complete set of explanatory variables (full model), (c) both refined biophysical and anthropogenic variables (integrated model), (d) refined biophysical variables (natural model), and (e) refined anthropogenic variables (human model), respectively.

variable, contributing 6.1% to fire risk (Figures 5 and 6d). The response of fire probability to elevation also followed a bell shape (Figure 6e), with a peak at 700–800 m and decrease at lower and higher elevation. The national fire danger rating system's (NFDRS) burning index, an integrated meteorological indicator of fire danger (Mees & Chase, 1991), contributed 5.4% to fire probability (Figure 5), with higher burning index associated with higher fire probability (Figure 6f).

Other biophysical variables such as PDSI, 100-h dead fuel moisture, and slope were less important for predicting the spatial distribution of fire probability, each with a relative contribution of less than 6% (Figure S5).

3.4. Importance of Anthropogenic Controls

Population density was the second most important predictor in the integrated model with a relative contribution of 15.8% (Figure 5). Fire probability decreased rapidly with increasing population density (Figure 6c), indicating that less densely populated areas had a higher fire risk. Additional metrics of human activity, such as minor road density or travel time, typically contributed less than 2% (Figure S5). Interestingly, minor roads and trail roads were more important than major roads and railways in the integrated model (Figure S5), probably due to their role in increasing access to wildlands.

3.5. Difference of Spatial Controls on Fire Probability Across Subecoregions

The patterns of fire risk predicted with separate MaxEnt integrated models built for each one of the five subecoregions (Figure 7) were consistent with the FRAP-based fire records (Figure 2a). Higher fire risk was predicted in lower and middle montane forests (Figures 7a and 7b), which is consistent with the FRAP-based fire records (Figure 2a). Fire risk was much lower in upper montane forests (Figure 7c), where a few hotspots were located in the south. Subalpine forests and alpine areas experienced a low fire risk (Figure 7d). A hotspot of fire risk was identified along the eastern slope of the southwest Sierra Nevada (Figure 7e). Although the derived spatial pattern of fire probability based on the subregions (Figure 7) was similar to that predicted by the single model developed for the entire Sierra Nevada (Figure 3b), the subecoregion based predictions achieved better performance in capturing finer-scale local variation in fire risk, for example, in lower montane forests (Figure 7a), middle montane forests (Figure 7b), and upper montane forests (Figure 7c).

Population density was the dominant control (33.1%) on the spatial variability of fire risk in lower montane forests, followed by 100-h dead fuel moisture (12.2%; Table 3). Population density (26.4%) and 100-h dead fuel moisture (23.9%) were equally important drivers, followed by PDSI (8%) in Middle montane forests. In con-
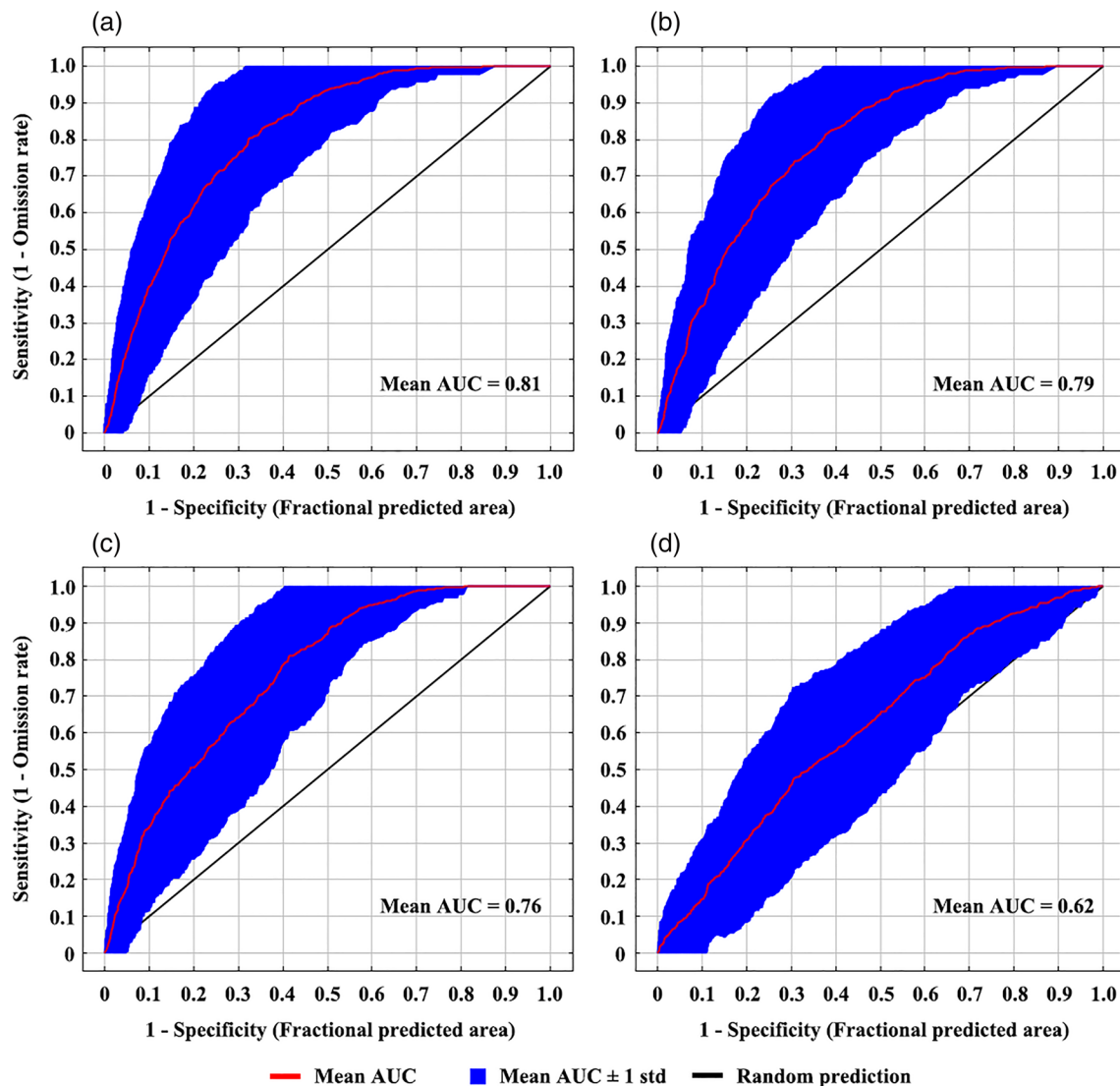
Figure 4. The receiver operating characteristic (ROC) curves for out-of-sample predictions from the MaxEnt-based fire probability models: (a) full model with the complete set of explanatory variables, (b) full model with both refined biophysical and anthropogenic variables, (c) natural model with refined biophysical variables, and (d) human model with refined anthropogenic variables.

trast, the burning index (20.2%) was the most important for fire variability in the Upper montane forests, while mean VPD (84.3%) predominantly controlled fire risk in Subalpine forests and Alpine areas. PDSI (28.8%) and mean VPD (23.5%) were comparably important variables in controlling fire risk on the Great Basin slope.

4. Discussion

4.1. Controls of Climate, Fuels, and Humans on Fire Risk

Climate variables, especially annual mean VPD, wind speed, and burning index were important drivers in explaining the spatial patterns of fire occurrence across the Sierra Nevada (Figure 5), as well as for individual subecoregions (Table 3). Mean VPD was the most important predictor for fire probability. Our findings are consistent with a recent study focusing on California that concluded nearly all of the 1972–2018 increase in summer forest-fire area was driven by increased VPD (Williams et al., 2019). We also found that NPP, which we interpret as an indicator of fuels, enhanced fire risk across the region (Figures 5 and 6). NPP varies with elevation in the Sierra Nevada, with decreasing NPP at higher elevation (Figure S6). Likewise,
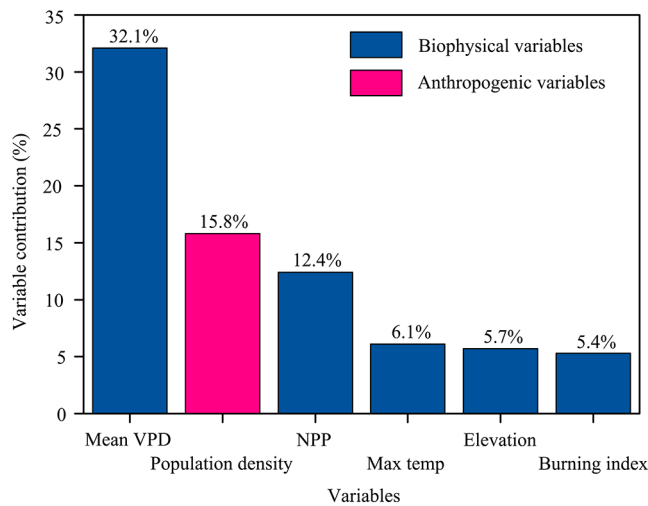
Figure 5. The relative contribution of top six variables to fire probability, based on results from the integrated model.

the response of fire probability to elevation showed that fire probability decreases at higher elevation (Figure 6e). These mechanisms contribute to the spatial pattern of fire probability predicted in our model, with the most fire prone areas at low to mid-elevations (Figure 2). For example, the Stanislaus National Forest in the central Sierra Nevada was a fire hot-spot (Figures 1c and 3), with a high predicted and observed fire occurrence, including the 2013 Rim fire (Peterson et al., 2015). This area is less populated, with an intermediate VPD value and a high NPP (Figure S6); these properties are predictive of particularly fire prone areas (Figure 6).

Our results are consistent with the interpretation that both ends of the climatic spectrum lead to reduced wildfire. For example, at the high el-evation, subalpine forests and alpine areas rarely experience coincided hot and dry weather, resulting in lower fire risk (Figure 7). On the other hand, some areas on the eastern Sierra slopes were too arid to support contiguous fuels, leading to limited wildfires (Figure 7). Areas with inter-mediate climate, such as lower, middle, and upper montane forests, had higher NPP and accumulated fuels, leading to higher fire probabilities.

This study showed considerable human impacts on fire probability, al-though the majority of Sierra Nevada has extensive wildlands and overall low-population density. For example, the relative importance analysis of all natural and anthropogenic variables revealed that population density was the second leading predictor of fire probability. The negative impact of population density presumably reflected the effect of increased suppression and fuel abatement near populated areas. Similarly, areas with better access, as indicated by shorter travel time (i.e., accessibil-ity to the nearest densely populated area), had lower fire probabilities (Figure S8). However, the density of major/minor roads and trail roads had a contrasting impact, that is, a sparser major/minor road network increased fire probability (Figure S8). This likely reflects the concentration of major/minor roads near more populated areas, and possibly also the effects of enhanced accessibility leading to improved suppression.
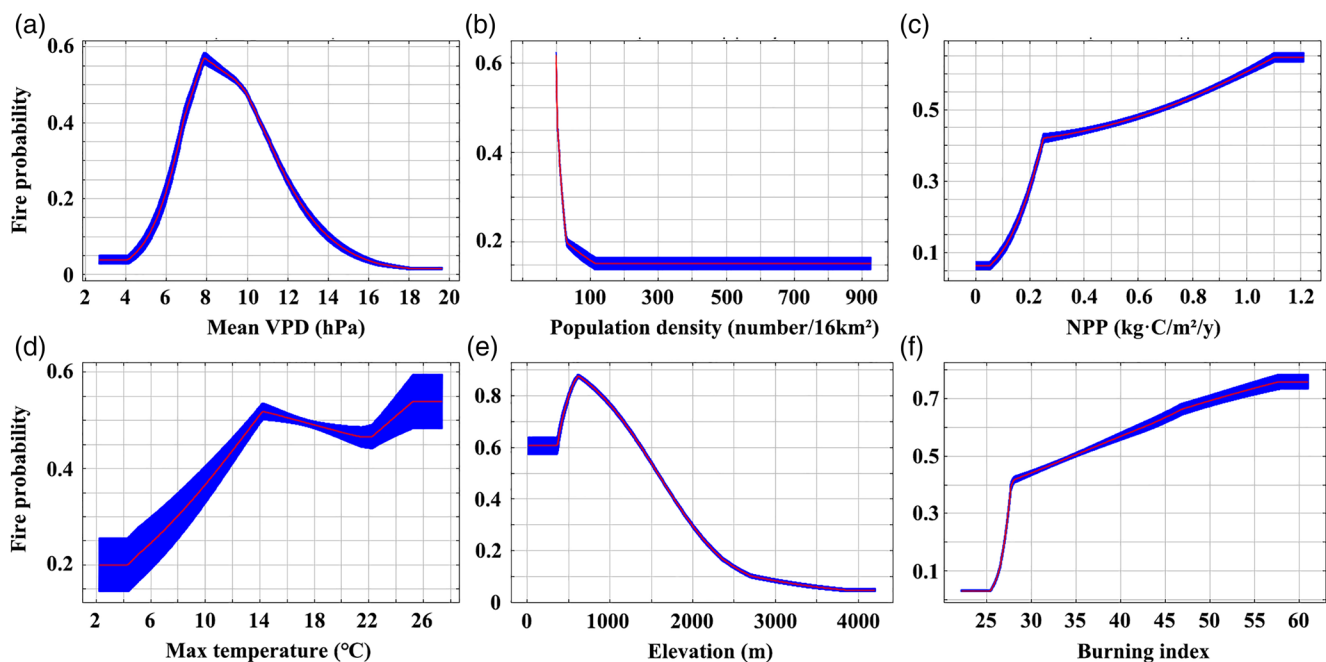
Figure 6. Partial dependence of fire probability on top six variables: (a) mean vapor pressure deficit, (b) population density, (c) net primary productivity, (d) maximum temperature, (e) elevation, and (f) burning index. The mean marginal response, that is, other variables were kept constant, is shown as the red curve, while the standard deviation as blue shades, based on the 100 replicates of the MaxEnt runs.
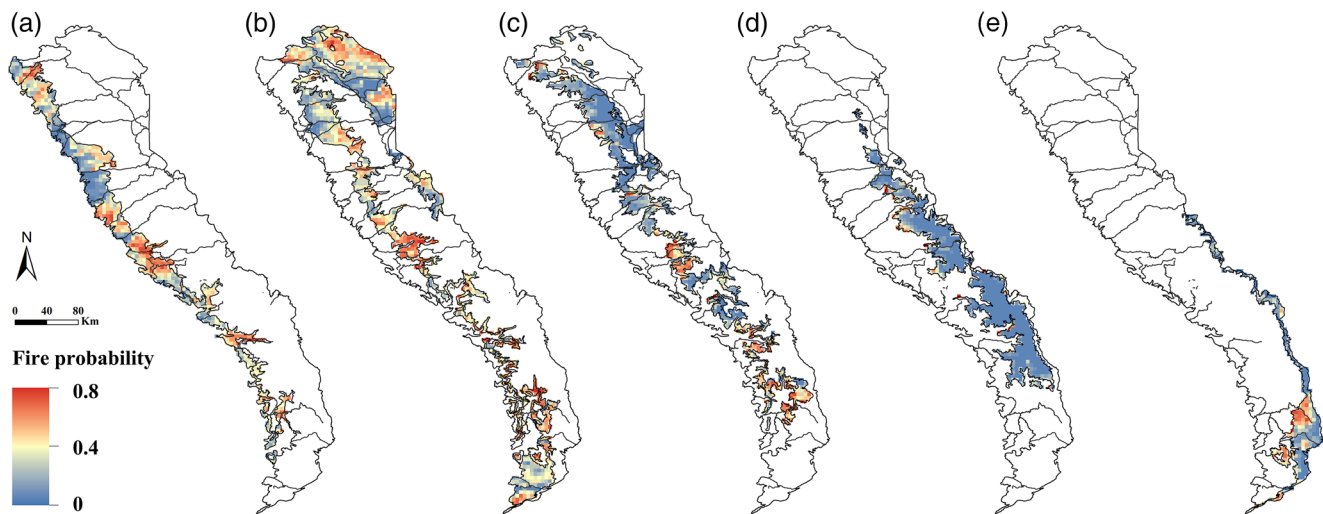
Figure 7. Fire risk predicted by the MaxEnt models developed for each subecoregion (a) lower montane forests, (b) middle montane forests, (c) upper montane forests, (d) subalpine forests and alpine areas, and (e) Great Basin slopes overlaid with major roads (black lines), using the integrated model by averaging out-of-sample predictions from 100 repeated model outputs.

Conversely, trail roads are associated with more remote wildlands, with statistically enhanced fire risks. Rail lines had a minimal effect due to their limited coverage (Figure S8).

This study addressed a few research gaps about more localized drivers shaping the spatial variability of contemporary wildfire burn probability in the Sierra Nevada. Partitioning Sierra Nevada into subecoregions provides additional information about more localized wildfire controls. Our results showed that spatial distribution of fire probability was controlled by both biophysical and anthropogenic variables, and the relative importance differed across subecoregions. Human impacts were comparatively important at lower elevation. For example, population density is the first and second leading predictor for lower montane forests and middle montane forests regions, respectively. In contrast, influence from humans became much weaker at higher elevation. It therefore advanced our understanding of climate, fuel, and land use controls on the spatial pattern of wildfire at a finer scale in California's Sierra Nevada and how they vary among various subecoregions, which is critically important for developing effective fire management practices, while most previous studies focused on very coarse larger scales, either state or continental levels.

4.2. Management Implications

The out-of-sample predictions by the MaxEnt model provide an estimate of fire-presence probability at a 4 km resolution and may prove useful for fire mitigation. Climate warming over recent decades has in-

Table 3
Variable Importance for Spatial Variability of Fire Risk in Different Subecoregions of the Sierra Nevada

	Lower mountain forests	Middle mountain forests	Upper montane forests	Subalpine forests/ Alpine	Great Basin slopes
Variable contribution	Population density (33.1%)	Population density (26.4%)	Burning index (20.2%)	Mean VPD (84.3%)	PDSI (28.8%)
Variable contribution	100-h dead fuel moisture (12.2%)	100-h dead fuel moisture (23.9%)	100-h dead fuel moisture (14.8%)	Major roads (3.7%)	Mean VPD (23.5%)
Variable contribution	Travel time (10.0%)	PDSI (8.0%)	PDSI (14.7%)	Burning index (3.6%)	Wind speed (13.8%)
Variable contribution	PDSI (6.6%)	Travel time (7.3%)	NPP (11.2%)	Elevation (2.1%)	NPP (10.7%)
Variable contribution	Major roads (4.9%)	NPP (6.0%)	Mean VPD (7.9%)	Trail roads (2.1%)	Burning index (7.7%)

Results are shown for five most important variables for each subecoregion, ordered by variable importance from upper to bottom. NPP, Net primary production; PDSI, Palmer drought stress index; VPD, Vapor pressure deficit.

creased California's atmospheric VPD (Williams et al., 2019); this trend is expected to continue over the coming decades (Solomon et al., 2009; Wilson et al., 2016). The relationship we found between VPD and fire occurrence supports the notion that the intensified atmospheric aridity will increase fire risk, especially in upper and subalpine montane regions (Table 3).

Higher NPP leads to higher fire risks, suggesting that fuel management may be effective in reducing fire risk in this region. Fuel treatments such as thinning and removal, and prescribed fire are widely recognized as reducing fire risk and severity (Safford et al. 2009, 2012; Vaillant et al., 2009). The legacy of past fire suppression beginning in the late nineteenth and early twentieth centuries, has led to increased fuel loads in many forest ecosystems (Schoennagel et al., 2004; Westerling et al., 2006). Warming temperatures, intensified drought, and increasingly variable moisture conditions further impact fuel drying and accumulation, potentially triggering more frequent and severe fires. The mapped fire-presence probability in this study could be coupled with information on fuels to better support management, with an emphasis on high fire risk areas. Additionally, the derived fire risk map, which integrates multisource geospatial data layers that characterize fire activities, human, climatic and physical influences, provides a spatially explicit alternative to highlight where and why fire management strategies may be pursed in the context of ongoing and future climate change.

4.3. Uncertainties of the Approach

MaxEnt predicts wildfire likelihood by searching for the probability distribution with the maximum entropy, subject to the inclusive explanatory variables at each fire-presence sample. It is worth noting that MaxEnt can potentially capture the complex, nonlinear, and interacting effects of independent variables, as shown by Parisien and Moritz (2009). However, it may not be thought of as a causality-based approach. MaxEnt cannot separate the indirect causes of correlation from the direct causes, and we therefore used variable importance and partial dependence analysis to help interpreting the impact of climate, fuels, and humans on fire likelihood. For example, we do not believe the comparatively tight relationship between VPD and wildfire probability we observed (Figure 6a) fully reflects the direct effect of VPD on fire, but rather a covarying limitation of fuel in dry, warm, high VPD areas, and cold, wet, low VPD areas. The geographic distribution of VPD clearly showed that higher VPD values were mainly distributed at lower elevations and the Great Basin, which coincided with areas that had very limited fuel amounts (Figures S6 and S7). In contrast, the systematic increase in burning with NPP appears to reflect the direct control on wildfire probability as mediated by the relationships between primary production and fuel load. The relationship between population density and fire probability presumably reflects a suite of mechanisms, including the trade-off between more human-caused ignitions and more aggressive suppression. A further exploration of the casual links between geospatial predictors and wildfire probability is needed.

Although a large group of explanatory variables is not necessarily an obstacle for the prediction reliability of MaxEnt model, that is, the accuracy of AUC did not change much before and after refining inclusive variables in Figures 4a and 4b, the presence of highly correlated variables within the same category of biophysical and anthropogenic controls (Figures 2b and 2c) may nonetheless hinder model interpretation such as variable importance (Phillips et al., 2006). Meteorological variables such as maximum, minimum, and mean temperature and VPD exhibited high correlation (Figure 2b), since temperature is one of the key inputs to calculate VPD. Some GRIDMET variables showed high correlations, perhaps in part due to inaccurate quantification of meteorological heterogeneity (Daly et al., 2008). We addressed this collinearity issue by refining our analysis to exclude predictors that were highly correlated, in order to improve our understanding of the functional relationships between explanatory variables and wildfire probability.

We further tested the sensitivity and robustness of the MaxEnt model and variable importance to fire probability threshold for selecting fire-presence samples, by varying the cut-off threshold from 0.06 to 1.0 (Table S1). The higher threshold of fire probability led to a lower number of fire-presence samples (i.e., the sample size declines from 1,050 to 130 positive fire grid cells out of a domain total of 3,310 grid cells), but resulted in a better prediction performance (i.e., AUC from 0.69 to 0.87) because of the higher quality of fire-presence training samples. The relative contributions of various predictors were stable across all models trained with samples from different fire probability thresholds (Table S1). For example, annual mean VPD was always the predominant spatial control, and population density was consistently important among the anthropogenic variables. Given the spatial autocorrelation in wildfire occurrence, the true fire-presence

sample size will be smaller than the number of points we identified. The limited sample size and relatively high number explanatory variables that we examined may potentially lead to model overfitting. To address this issue, we reduced the number of driver variables in our refined set of MaxEnt models, and also assigned a more relaxed threshold of fire-presence to increase the sample size.

A few remaining caveats caused by data limitations need to be acknowledged. First, there was a slight mismatch between the temporal periods of some biophysical and anthropogenic variables and fire history used in this study (1984–2017). For example, the record of lightning strikes was from 1988 to 2012, while several transportation layers derived from Open Street Maps such as major, minor, and track roads represented a more recent state of the transportation network. Additionally, some of the anthropogenic variables were not complete in some areas, for example, powerlines. Second, the remote sensing based NDVI or NPP for the 30 m pixels that got burned during 1984–2017 was affected by fire disturbance. However, the prediction of fire burn probability in this study is more focused on spatial pattern at 4 km averaged from 1984 to 2017. The averaging of aggregated annual maximum of vegetation variables to long-term annual means at 4-km further reduced the short-term abrupt changes from fires. Third, to be consistent with the spatial resolution of climatic variables from PRISM and GRIDMET data sets, the minimum cell size used to map fire probability in this study was set to be 4 km. However, this spatial resolution remains too coarse to fully represents landscape heterogeneity, especially for the diverse vegetation types in the Sierra Nevada. Lastly, this study focused on the spatial variability of wildfire burn probability and thus did not take account of temporal changes of wildfires and the associated drivers. To be consistent with the mean burn probability, the corresponding drivers such as climatic and anthropogenic factors were also averaged during the 1984–2017 study period. However, we recognized that there was an increasing trend in temperature and VPD, which was found contributing to the increased wildfires and burned areas in California from 1972 to 2018 (Williams et al., 2019). In addition, the expanding WUI and intensified human modification also posed more wildfire threats to the housing community and natural ecosystems (Radeloff et al., 2018). Our next step is to build a dynamic fire probability model to integrate both the spatial and temporal biophysical and anthropogenic variables, which will provide a more comprehensive understanding about how wildfire probability changes in space and time.

5. Conclusions

We investigated how a set of comprehensive biophysical and anthropogenic factors determined the 4 km spatial variation of fire probability in California's Sierra Nevada mountains and across its subecoregions via MaxEnt models. The results showed that a model that included both biophysical and anthropogenic predictors best predicted fire probability (i.e., AUC = 0.81), while anthropogenic-only and biophysical-only models performed much less well. Model diagnostics of the relative contribution showed that biophysical variables were the most important for predicting fire probability, with annual mean VPD identified as the leading predictor. Population density and fuel amount also regulated the spatial patterns significantly, each accounting for 15.8%–12.4% of the relative contributions. The relative importance of biophysical and anthropogenic predictors differed across the five main subecoregions of the Sierra Nevada, with population density playing a particularly important role in lower-elevation montane forests, and burning index and annual mean VPD in higher-elevation montane forests. This study highlighted the varying importance of climatic and human controls for spatial variation of fire probability across the Sierra Nevada, and carried implications for region-specific forest management strategies to limit future increases in wildfire risks.

Data Availability Statement

All data used in this study are publicly available. The California Fire and Resource Assessment Program (https://frap.fire.ca.gov/mapping/gis-data/) provides fire perimeter database. Monthly climate data are available from the PRISM Climate Group (http://www.prism.oregonstate.edu/), and daily climate data from the Climatology Lab (http://www.climatologylab.org/gridmet.html). Monthly lightning-strike data are from the NOAA Vaisala National Lightning Detection Network (https://www.ncdc.noaa.gov/data-access/severe-weather/lightning-products-and-services). Vegetation data from Landsat and MODIS and topographic data are from the Google Earth Engine data archive (https://earthengine.google.com/). Human settlement layers are available from the European Commission-Global Human Settlement

(https://ghsl.jrc.ec.europa.eu/). The Gridded Population of the World are available https://sedac.ciesin. columbia.edu/data/collection/gpw-v4/. OpenStreetMap (https://www.openstreetmap.org/) provides road network, mining production and powerline data layers. Human modification layer and travel time layer are available from the Google Earth Engine data archive (https://earthengine.google.com/; Kennedy et al., 2019; Weiss et al., 2018). The MaxEnt model software is available (https://biodiversityinformatics. amnh.org/open_source/maxent/).

References

Abatzoglou, J. T. (2013). Development of gridded surface meteorological data for ecological applications and modelling. *International Journal of Climatology*, *33*, 121–131.

Abatzoglou, J. T., Barbero, R., Wolf, J. W., & Holden, Z. A. (2014). Tracking interannual streamflow variability with drought indices in the US Pacific Northwest. *Journal of Hydrometeorology*, *15*, 1900–1912.

Balch, J. K., Bradley, B., Abatzoglou, J. T., Nagy, C., Fusco, E., & Mahood, A. (2017). Human-started wildfires expand the fire niche across the United States. *Proceedings of the National Academy of Sciences*, *114*, 2946.

Brewer, M. J., & Clements, C. B. (2020). The 2018 Camp Fire: Meteorological analysis using in situ observations and numerical simulations. *Atmosphere*, *11*, 47.

Butsic, V., Kelly, M., & Moritz, M. A. (2015). Land use and wildfire: A review of local interactions and teleconnections. *Land*, *4*, 140–156.

California Department of Forestry and Fire Protection (2017). *California Fire and Resource Assessment Program (FRAP) (version 17_1) fire perimeter data*. California Department of Forestry and Fire Protection.

Calkin, D. E., Cohen, J. D., Finney, M. A., & Thompson, M. P. (2014). How risk management can prevent future wildfire disasters in the wildland-urban interface. *Proceedings of the National Academy of Sciences*, *111*, 746–751.

Caprio, A. C., & Swetnam, T. W. (1995). *Historic fire regimes along an elevational gradient on the west slope of the Sierra Nevada* (pp. 173–179). CA: United States Department of Agriculture Forest Service General Technical Report Int.

Chen, B., Jin, Y., & Brown, P. (2019). Automatic mapping of planting year for tree crops with Landsat satellite time series stacks. *ISPRS Journal of Photogrammetry and Remote Sensing*, *151*, 176–188. https://doi.org/10.1016/j.isprsjprs.2019.03.012

Collins, B. M., & Stephens, S. L. (2007). Managing natural wildfires in Sierra Nevada wilderness areas. *Frontiers in Ecology and the Environment*, *5*, 523–527.

Dai, A., Trenberth, K. E., & Qian, T. (2004). A global dataset of Palmer Drought Severity Index for 1870–2002: Relationship with soil moisture and effects of surface warming. *Journal of Hydrometeorology*, *5*, 1117–1130.

Daly, C., Halbleib, M., Smith, J. I., Gibson, W. P., Doggett, M. K., Taylor, G. H., et al. (2008). Physiographically sensitive mapping of climatological temperature and precipitation across the conterminous United States. *International Journal of Climatology: A Journal of the Royal Meteorological Society*, *28*, 2031–2064.

Danielson, J., & Gesch, D. (2011). *Global multi-resolution terrain elevation data 2010*. US Department of the Interior and US Geological Survey.

Dettinger, M. D., Alpert, H., Battles, J. J., Kusel, J., Safford, H., Fougeres, D., et al. (2018). *Sierra Nevada summary report. California's Fourth Climate Change Assessment*. California Energy Commission/Natural Resoources Agency.

DiMiceli, C. M., Carroll, M. L., Sohlberg, R. A., Huang, C., Hansen, M. C., & Townshend, J. R. G. (2017). *Annual global automated MODIS vegetation continuous fields (MOD44B) at 250 m spatial resolution for data years beginning day 65, 2000-2010*. University of Maryland, College Park.

Elith, J. (2000). Quantitative methods for modeling species habitat: Comparative performance and an application to Australian plants. In S. Ferson & M. Burgman (Eds.), *Quantitative methods for conservation biology* (pp. 39–58). New York, NY: Springer New York.

Elith, J., Phillips, S. J., Hastie, T., Dudík, M., Chee, Y. E., & Yates, C. J. (2011). A statistical explanation of MaxEnt for ecologists. *Diversity and Distributions*, *17*, 43–57.

Fusco, E. J., Abatzoglou, J. T., Balch, J. K., Finn, J. T., & Bradley, B. A. (2016). Quantifying the human influence on fire ignition across the western USA. *Ecological Applications*, *26*(8), 2390–2401.

Goulden, M. L., Anderson, R. G., Bales, R. C., Kelly, A. E., Meadows, M., & Winston, G. C. (2012). Evapotranspiration along an elevation gradient in California's Sierra Nevada. *Journal of Geophysical Research*, *117*. https://doi.org/10.1029/2012JG002027

Haight, R. G., Cleland, D. T., Hammer, R. B., Radeloff, V. C., & Rupp, T. S. (2004). Assessing fire risk in the wildland-urban interface. *Journal of Forestry*, *102*, 41–48.

Haklay, M. (2010). How good is volunteered geographical information? A comparative study of OpenStreetMap and ordnance survey datasets. *Environment and Planning B: Planning and Design*, *37*, 682–703.

Heinsch, F. A., Reeves, M., Votava, P., Kang, S., Milesi, C., Zhao, M., et al. (2003). GPP and NPP (MOD17A2/A3) products NASA MODIS land algorithm. In *MOD17 User's Guide* (pp. 1–57).

Kennedy, C. M., Oakleaf, J. R., Theobald, D. M., Baruch-Mordo, S., & Kiesecker, J. (2019). Managing the middle: A shift in conservation priorities based on the global human modification gradient. *Global Change Biology*, *25*. https://doi.org/10.1111/gcb.14549

Keyser, A. R., & Westerling, A. L. (2019). Predicting increasing high severity area burned for three forested regions in the western United States using extreme value theory. *Forest Ecology and Management*, *432*, 694–706.

Krawchuk, M., & Moritz, M. (2014). Burning issues: statistical analyses of global fire data to inform assessments of environmental change. *Environmetrics*, *25*, 472–481.

Mann, M. L., Batllori, E., Moritz, M. A., Waller, E. K., Berck, P., Flint, A. L., et al. (2016). Incorporating anthropogenic influences into fire probability models: Effects of human activity and climate change on fire activity in California. *PLoS ONE*, *11*, e0153589.

Mansuy, N., Miller, C., Parisien, M. A., Parks, S. A., Batllori, E., & Moritz, M. A. (2019). Contrasting human influences and macro-environmental factors on fire activity inside and outside protected areas of North America. *Environmental Research Letters*, *14*(6), 064007.

Mees, R., & Chase, R. (1991). Relating burning index to wildfire workload over broad geographic areas. *International Journal of Wildland Fire*, *1*(4), 235–238.

Miller, J. D., Safford, H. D., Crimmins, M., & Thode, A. E. (2009). Quantitative evidence for increasing forest fire severity in the Sierra Nevada and southern cascade mountains, California and Nevada, USA. *Ecosystems*, *12*, 16–32.

Miller, J. D., & Safford, H. (2012). Trends in wildfire severity: 1984 to 2010 in the Sierra Nevada, Modoc Plateau, and southern Cascades, California, USA. *Fire Ecology*, *8*, 41–57.

Miller, J. D., Skinner, C. N., Safford, H. D., Knapp, E. E., & Ramirez, C. M. (2012). Trends and causes of severity, size, and number of fires in northwestern California, USA. *Ecological Applications*, *22*, 184–203.

Moritz, M. A., Batllori, E., Bradstock, R. A., Gill, A. M., Handmer, J., Hessburg, P. F., et al. (2014). Learning to coexist with wildfire. *Nature*, *515*, 58–66.

Moritz, M. A., Parisien, M. A., Batllori, E., Krawchuk, M. A., Van Dorn, J., Ganz, D. J., & Hayhoe, K. (2012). Climate change and disruptions to global fire activity. *Ecosphere*, *3*, 1–22.

Openstreetmap (2017). www.openstreetmap.org

Parisien, M.-A., Miller, C., Parks, S. A., DeLancey, E. R., Robinne, F. N., & Flannigan, M. D. (2016). The spatially varying influence of humans on fire probability in North America. *Environmental Research Letters*, *11*, 075005.

Parisien, M.-A., & Moritz, M. A. (2009). Environmental controls on the distribution of wildfire at multiple spatial scales. *Ecological Monographs*, *79*, 127–154.

Parisien, M.-A., Snetsinger, S., Greenberg, J. A., Nelson, C. R., Schoennagel, T., Dobrowski, S. Z., et al. (2012). Spatial variability in wildfire probability across the western United States. *International Journal of Wildland Fire*, *21*, 313–332.

Pechony, O., & Shindell, D. T. (2010). Driving forces of global wildfires over the past millennium and the forthcoming century. *Proceedings of the National Academy of Sciences*, *107*, 19167–19170.

Pesaresi, M., Ehrlich, D., Ferri, S., Florczyk, A., Freire, S., Halkia, M., et al. (2016). *Operating procedure for the production of the global human settlement layer from Landsat data of the epochs 1975, 1990, 2000, and 2014* (1–62). Publications Office of the European Union.

Peterson, D. A., Hyer, E. J., Campbell, J. R., Fromm, M. D., Hair, J. W., Butler, C. F., et al. (2015). The 2013 Rim Fire: Implications for predicting extreme fire spread, pyroconvection, and smoke emissions. *Bulletin of the American Meteorological Society*, *96*, 229–247.

Phillips, S. J., Anderson, R. P., & Schapire, R. E. (2006). Maximum entropy modeling of species geographic distributions. *Ecological Modelling*, *190*, 231–259.

Phillips, S. J., Dudík, M., & Schapire, R. E. (2004). A maximum entropy approach to species distribution modeling. *Proceedings of the twenty-first international conference on Machine learning* (pp. 83). Banff, AB: ACM.

Radeloff, V. C., Hammer, R. B., Stewart, S. I., Fried, J. S., Holcomb, S. S., & McKeefry, J. F. (2005). The wildland–urban interface in the United States. *Ecological Applications*, *15*, 799–805.

Radeloff, V. C., Helmers, D. P., Kramer, H. A., Mockrin, M. H., Alexandre, P. M., Bar-Massada, A., et al. (2018). Rapid growth of the US wildland-urban interface raises wildfire risk. *Proceedings of the National Academy of Sciences*, *115*, 3314.

Restaino, J. C., & Peterson, D. L. (2013). Wildfire and fuel treatment effects on forest carbon dynamics in the western United States. *Forest Ecology and Management*, *303*, 46–60.

Safford, H. D., Schmidt, D. A., & Carlson, C. H. (2009). Effects of fuel treatments on fire severity in an area of wildland–urban interface, Angora Fire, Lake Tahoe Basin, California. *Forest Ecology and Management*, *258*, 773–787.

Safford, H. D., Stevens, J. T., Merriam, K., Meyer, M. D., & Latimer, A. M. (2012). Fuel treatment effectiveness in California yellow pine and mixed conifer forests. *Forest Ecology and Management*, *274*, 17–28.

San-Miguel-Ayanz, J., Moreno, J. M., & Camia, A. (2013). Analysis of large fires in European Mediterranean landscapes: Lessons learned and perspectives. *Forest Ecology and Management*, *294*, 11–22.

Schoennagel, T., Veblen, T. T., & Romme, W. H. (2004). The interaction of fire, fuels, and climate across Rocky Mountain forests. *AIBS Bulletin*, *54*, 661–676.

Schwartz, M. W., Butt, N., Dolanc, C. R., Holguin, A., Moritz, M. A., North, M. P., et al. (2015). Increasing elevation of fire in the Sierra Nevada and implications for forest change. *Ecosphere*, *6*, 1–10.

Solomon, S., Plattner, G. K., Knutti, R., & Friedlingstein, P. (2009). Irreversible climate change due to carbon dioxide emissions. *Proceedings of the National Academy of Sciences*, *106*, 1704–1709.

Spracklen, D. V., Logan, J. A., Mickley, L. J., Park, R. J., Yevich, R., Westerling, A. L., & Jaffe, D. A. (2007). Wildfires drive interannual variability of organic carbon aerosol in the western US in summer. *Geophysical Research Letters*, *34*. https://doi.org/10.1029/2007GL030037

Stephens, S. L., Collins, B. M., Fettig, C. J., Finney, M. A., Hoffman, C. M., Knapp, E. E., et al. (2018). Drought, tree mortality, and wildfire in forests adapted to frequent fire. *BioScience*, *68*, 77–88.

Sullivan, E., Jackson, C., Broberg, D., O'Dair, M., & Velan, V. (2019). *California lawmakers should take action to mitigate the effects of the 2019 PG&E bankruptcy*. eScholarship, University of California.

Swetnam, T. W., Baisan, C. H., Morino, K., & Caprio, A. C. (1998). *Fire history along elevational transects in the Sierra Nevada, California. Final report to the Sierra Nevada global change research program*. University of Arizona, Laboratory of Tree-Ring Research.

Syphard, A. D., Radeloff, V. C., Keeley, J. E., Hawbaker, T. J., Clayton, M. K., Stewart, S. I., et al. (2007). Human influence on California fire regimes. *Ecological Applications*, *17*, 1388–1402.

Syphard, A. D., Rustigian-Romsos, H., Mann, M., Conlisk, E., Moritz, M. A., & Ackerly, D. (2019). The relative influence of climate and housing development on current and projected future fire patterns and structure loss across three California landscapes. *Global Environmental Change*, *56*, 41–55.

US Forest Service (2009). *CALVEG. Pacific southwest region*.

Vaillant, N. M., Fites-Kaufman, J. A., & Stephens, S. L. (2009). Effectiveness of prescribed fire as a fuel treatment in Californian coniferous forests. *International Journal of Wildland Fire*, *18*, 165–175.

Weiss, D. J., Nelson, A., Gibson, H. S., Temperley, W., Peedell, S., Lieber, A., et al. (2018). A global map of travel time to cities to assess inequalities in accessibility in 2015. *Nature*, *553*, 333–336.

Westerling, A. L. (2016). *Increasing western US forest wildfire activity: Sensitivity to changes in the timing of spring* (371). Philosophical Transactions of the Royal Society B: Biological Sciences.

Westerling, A. L., Gershunov, A., Brown, T. J., Cayan, D. R., & Dettinger, M. D. (2003). Climate and wildfire in the western United States. *Bulletin of the American Meteorological Society*, *84*, 595–604.

Westerling, A. L., Hidalgo, H. G., Cayan, D. R., & Swetnam, T. W. (2006). Warming and earlier spring increase western U.S. forest wildfire activity. *Science*, *313*, 940.

Whitman, E., Batllori, E., Parisien, M. A., Miller, C., Coop, J. D., Krawchuk, M. A., et al. (2015). The climate space of fire regimes in north-western North America. *Journal of Biogeography*, *42*(9), 1736–1749.

Williams, A. P., Abatzoglou, J. T., Gershunov, A., Guzman-Morales, J., Bishop, D. A., Balch, J. K., et al. (2019). Observed impacts of anthropogenic climate change on wildfire in California. *Earth's Future*, *7*, 892–910.

Wilson, T. S., Sleeter, B. M., & Cameron, D. R. (2016). Future land-use related water demand in California. *Environmental Research Letters*, *11*, 054018.